Giant Piezoelectric Effects in Monolayer Group-V Binary Compounds with Honeycomb Phases: A First-Principles Prediction

Huabing Yin,[†,‡] *Jingwei Gao,*[‡] *Guang-Ping Zheng,*[*,‡] *Yuanxu Wang,*[*,†] *and Yuchen Ma*[¶]

[†]Institute for Computational Materials Science, School of Physics and Electronics, Henan University, Kaifeng 475004, China

[‡]Department of Mechanical Engineering, The Hong Kong Polytechnic University, Hong Kong 999077, China

[¶]School of Chemistry and Chemical Engineering, Shandong University, Jinan 250100, China

ABSTRACT

Two-dimensional (2D) piezoelectric materials have gained considerable attention since they could play important roles in the nanoelectromechanical systems. Herein, we report a first-principles study on the piezoelectric properties of monolayer group-V binary compounds with theoretically stable honeycomb phases (α-phase and β-phase). Our calculations for the first time reveal that a majority of the monolayers possess extremely high piezoelectric coefficients d_{11}, i.e., 118.29, 142.44, and 243.45 pm/V for α-SbN, α-SbP, and α-SbAs, respectively, comparable to those of recently reported group-IV monochalcogenides (d_{11} = 75−250 pm/V) with an identical *mm2* symmetry. It is found that the giant piezoelectric responses of α-phase monolayers as compared to those of β-phase monolayers are induced by their flexible structures and special symmetry. Meanwhile, the piezoelectric coefficients of α-phase monolayers are found to be surprisingly anisotropic and obey a unique periodic trend which is not exactly identical to that for the β-phase monolayers. To gain a comprehensive understanding of the periodic trends in piezoelectricity, several factors which influence the piezoelectric coefficients are quantitatively determined.

INTRODUCTION

Since the discovery of graphene in 2004,[1] a series of two-dimensional (2D) layered materials beyond graphene have been designed and fabricated. Those 2D materials, ranging from insulators to semiconductors and metals, exhibit unique properties and application perspectives as compared with those of their three-dimensional (3D) counterparts.[2-5] Studies on the intrinsic properties of 2D monolayer materials are important and helpful for promoting their application and development in nano-devices. As revealed by recent experimental and theoretical studies, many 2D monolayer materials, which are non-centrosymmetric, exhibit considerable piezoelectricity and are much promising for applications in sensors, actuators, and energy conversion devices.[6-13] By virtue of their unique crystal structures, 2D monolayer hexagonal boron nitride (*h*-BN) and a family of transition-metal dichalcogenides (TMDCs) were firstly selected to theoretically examine their piezoelectric effects.[6, 10, 12, 14] More notably, the piezoelectric coefficient (e_{11} = 2.9 × 10^{-10} C/m) of monolayer MoS_2 measured by subsequent experiment[8] confirmed the previous theoretical prediction with a calculated value of e_{11} = 3.64 × 10^{-10} C/m.[12] Notwithstanding, 2D materials with larger piezoelectric coefficients are desirable since their feasibility and applicability in sensors, actuators and energy conversion devices could be much improved.

Recently, many new one-atom-thick and few-atom-thick monolayer materials, including metal oxides,[10, 15] group-II,[10-11] -III,[16-17] and -IV monochalcogenides,[13] and group-III-V compounds,[10, 18] have been predicted to be piezoelectric by theoretical calculations and thus greatly enrich the existing knowledge of the family of 2D piezoelectric materials. A majority of them possess high piezoelectric coefficient d_{11}, which is the most useful coefficient in

determining the efficiency of mechanical-to-electrical energy conversion. For example, a series of theoretical investigations have shown that Janus $GaInS_2$ and In_2SSe,[17] buckled GaS, [11] BaTe,[11] and CdO [10] monolayers exhibit remarkable piezoelectric responses with coefficients d_{11} of 8.33, 8.47, 18.66, 19.92, and 21.7 pm/V, respectively, which are all larger than those of *h*-BN, monolayer MoS_2, and most of bulk piezoelectric materials commonly used to date.[12, 19-20] In particular, as observed by Fei *et al.* and Hu *et al.* using first-principles simulations, monolayer group-IV monochalcogenides with α-phase and γ-phase, e.g., GeS, GeSe, SnS, and SnSe, are strongly piezoelectric. The calculated relaxed-ion piezoelectric coefficients d_{11} of γ-phase and α-phase GeS, GeSe, SnS, and SnSe are as high as 20−91 pm/V and 75−250 pm/V, respectively.[13, 21] All those theoretical studies have pointed out the directions for the future development of 2D piezoelectric materials with giant piezoelectricity, while more experimental results are needed to verify the calculations.

Since 2014, 2D few-layer black phosphorus sheets have been successfully isolated from the bulk by mechanical and liquid exfoliation methods.[22-24] Other few-layer structures of group-V elements, including phosphorene, arsenene, and antimonene, have been brought into the family of 2D layered materials.[25-34] Unlike graphene, these systems possess non-zero band gaps, high carrier mobility, obvious anisotropy.[29] By theoretical method, Zhang *et al.* further investigated a class of possible monolayer group-V allotropes and proposed that two types of layered phases, i.e., α-phase and β-phase, have the best energetic stability.[29] In experiments, beside phosphorene, few-layer antimonene and arsenene nanoribbons have also been synthesized by various technologies and the stable structures predicted by theoretical calculations have been verified by relevant experimental results.[31-32, 35] Obviously, one-element group-V monolayers with an α-phase or β-phase have no intrinsic piezoelectricity since their crystal structures are

centrosymmetric. In order to change the structure symmetry and enhance the piezoelectricity of group-V monolayers, following the examples of other 2D alloying materials, it is feasible that the stable group-V monolayers could be composed into binary compounds, e.g., α-AsP alloy,[36-37] which have been synthesized with various chemical compositions and mechanically exfoliated down to several atomic layers.[38] Meanwhile, a series of monolayer group-V binary compounds with either α-phase or β-phase, i.e., PN, AsN, SbN, AsP, SbP, and SbAs, have been predicted to possess excellent energetic stability and electronic properties.[39-48] Since the α-phase and β-phase binary compounds have the *mm2* (or C_{2v}) and *3m* (or C_{3v}) point-group symmetry, respectively, the non-zero independent piezoelectricity could appear in these systems. Nonetheless, there is a lack of detailed study on the piezoelectricity of monolayer group-V binary compounds and thus relevant theoretical calculations could provide some valuable information about the piezoelectric effects in those 2D materials.

In this work, based on first-principles density functional theory (DFT), we systematically investigated the intrinsic piezoelectricity of stable monolayer phases of group-V binary compounds, including PN, AsN, SbN, AsP, SbP, and SbAs. We showed that all these monolayer materials with either α-phase or β-phase were piezoelectric. Surprisingly, the α-phase monolayer structures of group-V binary compounds exhibited remarkable and anisotropic piezoelectric properties and their piezoelectric coefficients d_{11} were determined to be as large as those of monolayer group-IV monochalcogenides (such as SnSe, SnS, GeSn, and GeS), which were recently predicted to be strongly piezoelectric. Our theoretical results thus suggested that the monolayer systems of group-V binary compounds could be much promising in the development of efficient nano-sized sensors and energy conversion devices.

COMPUTATIONAL DETAILS

We perform first-principles calculations in a DFT-based framework as implemented in the VASP code with a projected augmented wave (PAW) method and a plane-wave energy cutoff of 500 eV.[49-51] For the exchange-correlation potential, the generalized gradient approximation (GGA) within the Perdew-Burke-Ernzerhof (PBE) formalism is employed.[52] In all calculations, the Brillouin zone is sampled using a regular $10 \times 15 \times 1$ Monkhorst-Pack k-point mesh.[53] The convergence criterion of electronic self-consistent field calculations is set as 10^{-6} eV for energy. Firstly, the lattice constants of 2D systems under study are optimized until the forces are less than 0.01 eV/Å. Subsequently, in the system with fixed lattice constants, atomic positions are optimized until a much stricter convergence criterion of 0.002 eV/Å for forces is reached. Meanwhile, a vacuum space with a thickness of about 18 Å is added in the *z*-direction to avoid mirror interactions among atoms.

The elastic tensors of a relaxed-ion and clamped-ion system, with and without ionic contributions, are all calculated directly using the finite differences method in VASP,[54] which are generally in agreement with those calculated by another frequently used method for 2D materials, i.e, those calculated by fitting the unit-cell energy to a series of strain states.[10, 12] On the other hand, we calculate both relaxed-ion and clamped-ion linear piezoelectric coefficients of monolayer group-V binary compounds by using the modern theory of polarization based on the Berry's phase approximation.[55-56] According to the definitions, the third-rank piezoelectric tensors e_{ijk} and d_{ijk} can be evaluated by

$$e_{ijk} = \frac{dP_i}{d\varepsilon_{jk}}, \qquad (1)$$

$$d_{ijk} = \frac{dP_i}{d\sigma_{jk}}, \qquad (2)$$

where ε_{jk}, σ_{jk}, and P_i represent the strain tensor, stress tensor, and polarization tensor, respectively.[57] And the indices i=1, 2, and 3 for polarization tensor P_i indicate the polarization components along x-, y-, and z-directions, respectively. In Voigt notation,[57] for ε_{jk} and σ_{jk} tensors, the indices j and k can also be labeled as 1 = xx, 2 = yy, 3 = zz, 4 = yz, 5 = zx, and 6 = xy. However, in 2D materials, we only consider the in-plane strains and stresses, such as those with 1 (xx), 2 (yy), and 6 (xy) components. Therefore, the second-rank ε_{jk} tensors of quasi-2D systems under study can be indicated as only three forms, i.e., ε_{11}, ε_{22}, and ε_{12} , where 1 or 2 corresponds to x- or y-direction as defined in Figure 1 and the relationship of $\varepsilon_{12} = \varepsilon_{21}$ could exist.[12-13] It is known that the crystal symmetry decides the number of non-zero and independent piezoelectric coefficients. As shown in Figures 1a and 1b, the α-phase and β-phase monolayers of group-V binary compounds belong to *mm2* and *3m* point groups, respectively. Interestingly, the piezoelectric properties of 2D monolayers with these point-group symmetries have been analyzed by Duerloo *et al.*, Fei *et al.*, and Blonsky *et al.* particularly.[10, 12-13]

For α-phase structures with *mm2* point-group symmetry, the independent piezoelectric coefficients e_{11}, e_{12}, e_{26}, d_{11}, d_{12} and d_{26} are non-zero.[13] The coefficients e_{26} and d_{26} represent the piezoelectric effect of polarization along y-direction subjected to the applied shear strain on the xy-plane and here we specifically pay attention to the coefficients e_{11}, e_{21}, d_{11}, and d_{12}. Based on the relationship [57]

$$e_{ik} = d_{ij}C_{jk}, \qquad (3)$$

where C_{jk} is the elastic stiffness coefficients, we can obtain d_{11} and d_{12} from e_{11}, e_{12}, C_{11}, C_{22}, and C_{12} as [13]

$$d_{11} = \frac{e_{11}C_{22} - e_{12}C_{12}}{C_{11}C_{22} - C_{12}^2} , \qquad (4)$$

$$d_{12} = \frac{e_{12}C_{11} - e_{11}C_{12}}{C_{11}C_{22} - C_{12}^2} . \qquad (5)$$

Moreover, for β-phase structures with *3m* point-group symmetry, the non-zero and independent piezoelectric coefficients are e_{11}, e_{31}, d_{11}, and d_{31}. Using eq 3, similar to those of α-phase structures, d_{11} and d_{31} can be calculated as [10]

$$d_{11} = \frac{e_{11}}{C_{11} - C_{12}} , \qquad (6)$$

$$d_{31} = \frac{e_{31}}{C_{11} + C_{12}} . \qquad (7)$$

In the section that follows, we will carefully evaluate the piezoelectric effects in the monolayer group-V binary compounds with α-phase and β-phase by means of directly calculations on their piezoelectric coefficients.

RESULTS AND DISCUSSION

All calculations on the piezoelectric coefficients start from the optimized configurations of 2D monolayers and the corresponding α-phase and β-phase structures are shown in Figure 1. As predicted by previous theoretical studies,[41-43, 46-48] the two honeycomb phases of group-V binary

compounds (PN, AsN, SbN, AsP, SbP, and SbAs) are both very stable, owning to their greatly high cohesive energy. Meanwhile, the band structures of these monolayers have been reported systematically by DFT calculations accompanying by different exchange-correlation functionals, such as PBE and HSE06.[45-46] For α-phase structures, besides the *mm2* point-group non-centrosymmetric model with only one type of bond in the unit cell, as shown in Figure 1a, there may exist another centrosymmetric allotrope actually. Take α-SbAs for example, the centrosymmetric structure simultaneously possesses Sb-Sb, As-As, and Sb-As bonds in the unit cell. By examining the difference (~0.007 eV/atom) in formation energies of the two structures, we find that the non-centrosymmetric structure of α-SbAs has a little higher thermodynamic stability than the centrosymmetric one. For the β-phase structure which is hexagonal, it has only one independent lattice parameter (*a*) and there are two atoms in the primitive unit cell (Figure 1b). Nevertheless, in order to facilitate the calculations of elastic and piezoelectric properties, an orthorhombic super cell including four atoms is constructed for β-phase structures, similar to those for α-phase structures.

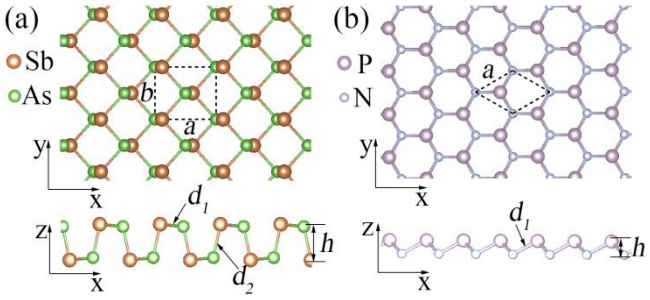

Figure 1. Optimized structures of (a) α-SbAs, and (b) β-PN binary compound monolayers from the top and side views. The α-SbAs and β-PN present orthorhombic and hexagonal structures, respectively, and their primitive unit cells are shown in dash boxes.

Table 1 summarizes the DFT-PBE calculated band gaps and geometrical parameters, which are defined in Figure 1, for all the 12 structures under study in this work. The results are generally in agreement with previous calculated values.[41-43, 46-48] Due to the increase of atomic radius, it is fairly easy to figure out that the geometrical parameters, including lattice constants, bond lengths, and monolayer thickness, increase roughly with the increasing atomic number for both α-phase and β-phase structures. Calculated by the same DFT-PBE method, the corresponding lattice parameters {*a, b*} of one-element monolayers of α-phase phosphorene, arsenene, and antimonene are {*a* = 4.53 Å, *b* = 3.36 Å}, {*a* = 4.76 Å, *b* = 3.69 Å}, and {*a* = 4.89, *b* = 4.35}, respectively.[29] And the lattice parameters *a* = 3.33 Å, 3.61 Å and 4.12 Å belong to β-phase phosphorene, arsenene, and antimonene, respectively.[29] The increase in bond lengths accompanied by covalence weakening in 2D compounds may induce the decrease of elastic stiffness coefficients. Besides, as listed in Table 1, all the 12 binary compounds are semiconducting materials with distinct band gaps, which are direct and indirect for α-phase and β-phase structures, respectively. The DFT-PBE band gaps of α-phase structures also show a periodic trend, which decrease from 2.18 eV for α-PN to 0.29 eV for α-SbAs. Similar trend in band gaps has also been demonstrated by Yu *et al.* previously,[46] but it is not so obvious for β-phase structures. It is worth noting that the PBE functional usually underestimates the band gaps of solids and more accurate and relatively higher values can be obtained by the *GW* method[58] or hybrid functional, e.g., HSE06.[59]

Table 1. DFT-PBE calculated lattice parameters (*a* and *b*), bond lengths (d_1 and d_2), monolayer thickness (*h*), and band gaps (E_g) for α-phase and β-phase monolayer group-V binary compounds.

Material	a (Å)	b (Å)	d_1 (Å)	d_2 (Å)	h (Å)	E_g (eV)
α-PN	4.16	2.70	1.72	1.82	1.90	2.18
α-AsN	4.18	2.96	1.90	1.95	2.13	1.91
α-SbN	4.19	3.30	2.10	2.11	2.42	1.90
α-AsP	4.69	3.50	2.38	2.39	2.35	0.90
α-SbP	4.43	3.91	2.62	2.56	2.85	0.71
α-SbAs	4.73	4.04	2.73	2.67	2.80	0.29
β-PN	2.73		1.79		0.86	1.81
β-AsN	2.97		1.96		0.96	1.98
β-SbN	3.27		2.14		1.01	1.68
β-AsP	3.46		2.39		1.32	1.86
β-SbP	3.73		2.59		1.41	1.75
β-SbAs	3.87		2.70		1.52	1.49

To determine the piezoelectric strain tensors, by carrying out the aforementioned finite differences method, we first calculate the elastic stiffness coefficients C_{11}, C_{22}, and C_{12} of α-phase and β-phase compounds. The coefficients under the relaxed-ion and clamped-ion conditions, which are determined with and without the full relaxation of atomic position, respectively, are summarized in Table 2, noting that C_{11} is the same as C_{22} for β-phase structures. The elastic stiffness coefficients of α-As monolayer, calculated directly by the finite differences method performed in VASP or through fitting the unit-cell total energy E_T to a series of 7×7 strain states ε based on the formula $C = (1/A)\,\partial^2 E_T/\partial\varepsilon^2$,[12, 60] are also listed in Table 2 for comparison. Obviously, two methods can provide nearly the same elastic stiffness coefficients, which are comparable to those previously reported by Kecik *et al.*[60] and Wang *et al.*.[61] From Table 2, it can be observed that the experimentally relevant relaxed-ion elastic stiffness coefficients always have smaller values as compared to the clamped-ion ones due to the smaller

inner stresses in the systems under the relaxed-ion condition. Such difference in relaxed-ion and clamped-ion elastic stiffness coefficients has also been discovered and discussed in many other 2D materials.[12-13, 16, 18] Furthermore, in systems varying from PN to SbAs, their elastic stiffness coefficients decrease generally for both α-phase and β-phase structures. It is noteworthy that the existence of very small elastic stiffness C_{11} and C_{12} of α-SbN, α-SbP, and α-SbAs monolayers may be ascribed to the distinct structural and electronic properties of these compounds. The detailed evaluation of elastic stiffness, as discussed above, can result in an accurate estimation on piezoelectric properties based on the relationships between the tensors C_{ij} and d_{ij}.

Table 2. Clamped-ion and relaxed-ion elastic stiffness coefficients C_{11}, C_{22}, and C_{12} of α-phase and β-phase group-V binary compounds calculated at the DFT-PBE level. The corresponding coefficients of α-As monolayer are also listed for comparison. The coefficients are all in units of N/m.

	Clamped-ion			Relaxed-ion		
Material	C_{11}	C_{22}	C_{12}	C_{11}	C_{22}	C_{12}
α-As	55.4	70.1	33.5	19.6	64.9	17.1
	55.8[a]	70.0[a]	33.4[a]	18.0[a]	64.7[a]	19.1[a]
				20[b]	55[b]	18[b]
				13.3[c]	70.3[c]	19.1[c]
α-PN	103.4	217.5	52.1	43.3	204.1	24.4
α-AsN	75.8	160.3	47.5	20.6	144.3	17.8
α-SbN	55.6	136.6	50.0	7.8	107.3	13.0
α-AsP	62.0	83.3	32.3	18.8	78.6	18.4
α-SbP	52.4	73.9	36.6	10.4	60.2	13.8
α-SbAs	46.6	62.5	35.0	8.8	49.9	14.6

β-PN	154.2	22.9	150.2	20.1
β-AsN	112.3	28.3	105.8	23.0
β-SbN	92.7	28.2	80.6	21.0
β-AsP	68.5	11.8	62.9	9.5
β-SbP	54.5	11.5	46.8	8.7
β-SbAs	48.5	10.7	40.8	8.0

[a.] Values are calculated by the formula $C = (1/A)\,\partial^2 E_T/\partial\varepsilon^2$. [b.] Values are obtained from ref 60.

[c.] Values are obtained from ref 61.

According to the definition of piezoelectric tensors e_{ij} in eq 2, we further calculate the e_{ij} coefficients of α-phase and β-phase group-V binary compounds by evaluating the polarization changes of a rectangular unit cell under applied uniaxial strains. This method, also known as Berry's phase technique,[55-56] has been widely and successfully employed in the research of piezoelectricity of 2D crystals previously.[12-13, 16, 18] Similar to elastic stiffness coefficients discussed above, the relaxed-ion and clamped-ion piezoelectric coefficients are calculated. Herein, the coefficients e_{11} and e_{12} of α-phase structures with an *mm2* point-group symmetry and e_{11} and e_{31} of β-phase structures with a *3m* point-group symmetry have to be calculated to obtain the coefficients d_{11}, d_{12} and d_{31}. More specifically, in this work, the coefficients e_{11} and e_{12} are determined by a linear fitting of 2D polarization changes ΔP_1 along *x*-direction with respect to the uniaxial strains ε_{11} and ε_{22} along the *x*- and *y*-direction, respectively. Likewise, the coefficient e_{31} which reflects the polarization changes ΔP_3 along *z*-direction under the applied strain ε_{11} along the *x*-direction, is also obtained through the linear fitting for ΔP_3 versus ε_{11}. As indicated in Figures 2 and 3, we perform all the clamped-ion and relaxed-ion polarization calculations under

11 average strain states for ε_{11} and ε_{22}, which range from −0.01 to 0.01. In this strain range, the relations between polarization changes and strains are found to be linear for the 2D α-phase and β-phase monolayers, except for α-SbAs. While our calculations show that the strain limits of such linear relation for α-SbAs are as small as ±0.005, as highlighted in Figures 2 and 3.

In particular, the relaxed-ion coefficients are further elucidated below since they are always related to experimental values. As shown in Figures 2c and 3c, the relaxed-ion piezoelectric coefficients e_{11} of α-phase and β-phase binary monolayers are all positive since the polarization changes along *x*-direction increase with increasing strain ε_{11}. On the contrary, the coefficients e_{12} of some α-phase binary monolayers are negative, as shown in Figure 2d. For β-phase structures, the group-V binary monolayers also exhibit out-of-plane piezoelectric effects with non-zero e_{31} and d_{31}. Nevertheless, as depicted in Figure 3d, the coefficients e_{31} are nearly one order of magnitude smaller than the in-plane coefficients e_{11}. Therefore, we can predict that the piezoelectric coefficients d_{31} of β-phase group-V binary monolayers could be relatively small.

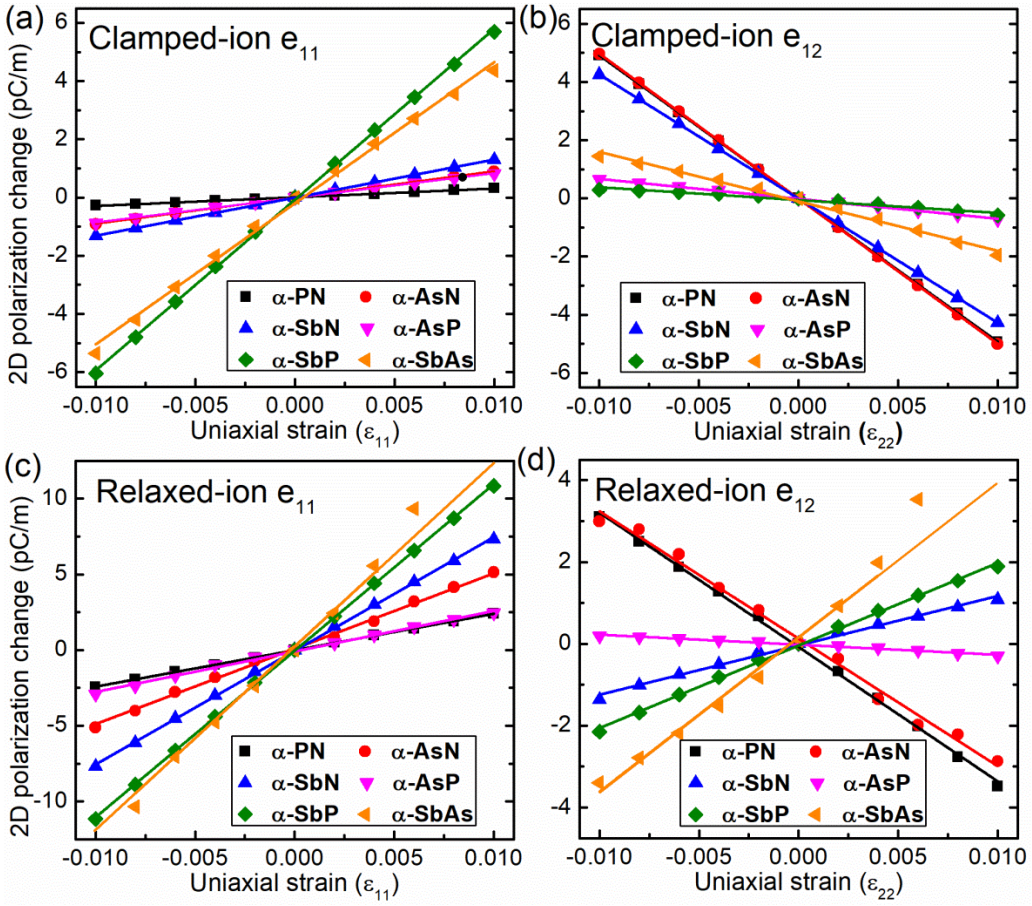

Figure 2. Calculated polarization changes per area along the *x*-direction under the applied uniaxial strains ε_{11} (a and c) and ε_{22} (b and d) along the *x*- and *y*-direction, respectively, for α-PN, α-AsN, α-SbN, α-AsP, α-SbP, and α-SbAs monolayers. The corresponding clamped-ion and relaxed-ion piezoelectric coefficients e_{11} and e_{12} can be obtained from the slopes of the lines.

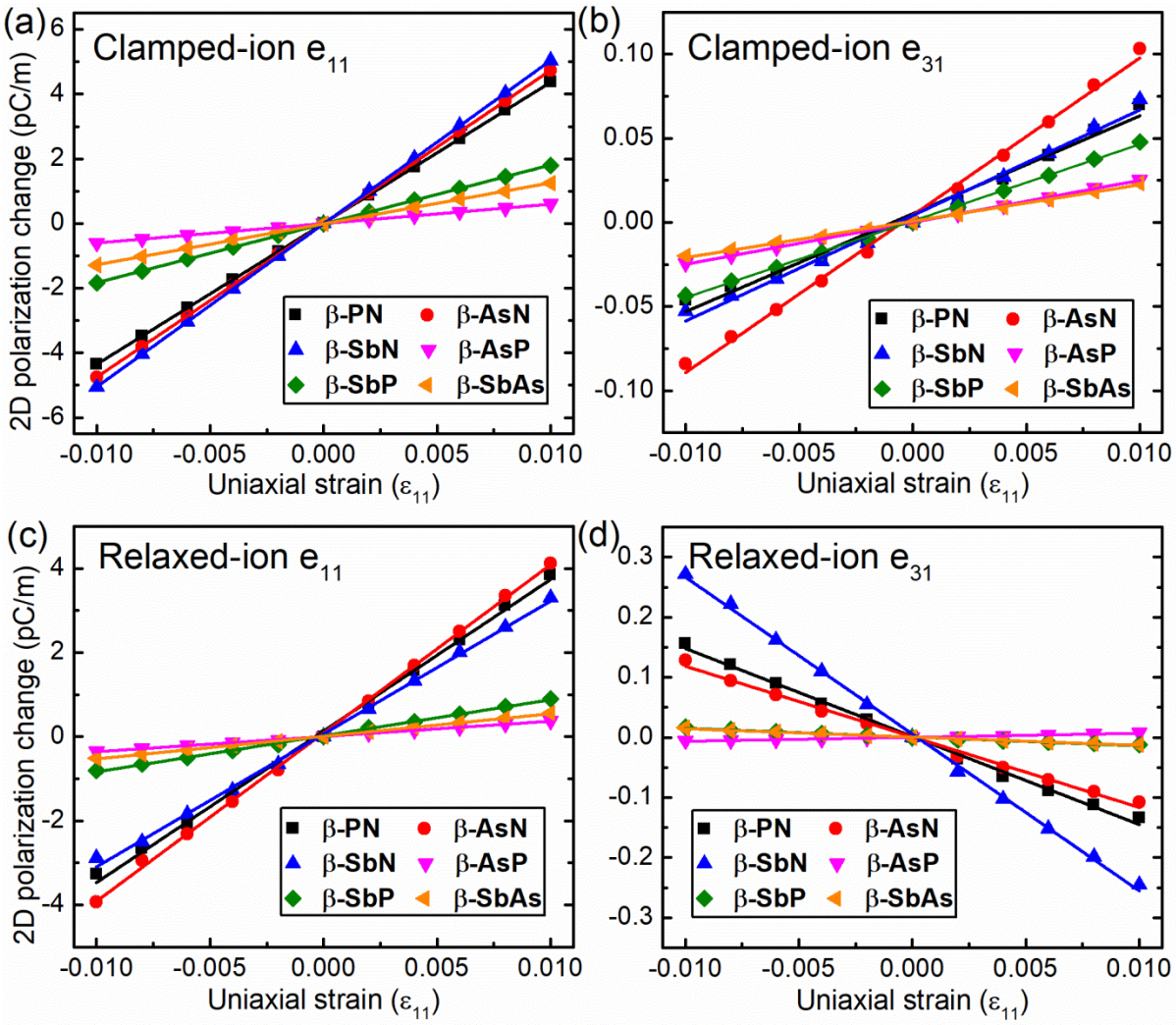

Figure 3. Calculated polarization change per area along the *x*- (a and c) and *z*-direction (b and d) under the applied uniaxial strain ε_{11} along the *x*-direction for β-PN, β-AsN, β-SbN, β-AsP, β-SbP, and β-SbAs monolayers. The corresponding clamped-ion and relaxed-ion piezoelectric coefficients e_{11} and e_{31} can be obtained from the slopes of the lines.

Once the piezoelectric coefficients e_{11}, e_{12} and e_{31}, and elastic stiffness coefficients C_{11}, C_{22} and C_{12} are obtained, based on eqs 4−7, we can determine the piezoelectric coefficients d_{11}, d_{12}

and d_{31}, which are important measures for the efficiency of mechanical-to-electrical energy conversion. All the relevant clamped-ion and relaxed-ion piezoelectric coefficients e_{11}, e_{12}, e_{31}, d_{11}, d_{12} and d_{31} calculated by DFT-PBE method for the α-phase and β-phase monolayer structures of group-V binary compounds, including PN, AsN, SbN, AsP, SbP, and SbAs, are summarized in Table 3. For all α-phase monolayers, it is found that the relaxed-ion coefficients e_{11} and d_{11} are much larger than their clamped-ion counterparts, consistent with those of 2D GeS, GeSe, SnS, and SnSe monolayers with the same symmetry.[13] The reason for that may be the ionic relaxation which releases some stresses in the unit cell. Similarly, as listed in Table 3, the relaxed-ion coefficients d_{12} of α-phase monolayers are larger than their clamped-ion counterparts, except for α-PN whose relaxed-ion coefficient (−2.44 pm/V) is a little smaller than the clamped-ion coefficient (−2.65 pm/V). Moreover, for β-phase structures, the calculated piezoelectric coefficients d_{31} confirm the above-mentioned prediction that they could be much small, e.g., the largest d_{31} is about −0.26 pm/V for β-SbN. Interestingly, in contrast to those of α-phase monolayers, the relaxed-ion coefficients d_{11} of β-phase monolayers are relatively smaller than those of the clamped-ion ones, as listed in Table 3. In general, for monolayer group-V binary compounds, the α-phase structures have stronger piezoelectricity than β-phase structures, which is attributed to the flexile puckered structures and unique electronic properties of α-phase monolayers. Similar conclusion was drawn for monolayer group-IV monochalcogenides.[13, 21]

Table 3. Calculated clamped-ion and relaxed-ion piezoelectric coefficients e_{11}, e_{12}, e_{31}, d_{11}, d_{12} and d_{31} of α-phase and β-phase monolayers of group-V binary compounds. The e_{11}, e_{12}, and e_{31} are in units of 10^{-10} C/m and d_{11}, d_{12}, and d_{31} are in units of pm/V.

	Clamped-ion						Relaxed-ion					
Material	e_{11}	e_{12}	e_{31}	d_{11}	d_{12}	d_{31}	e_{11}	e_{12}	e_{31}	d_{11}	d_{12}	d_{31}
α- PN	0.30	−4.92		1.63	−2.65		2.41	−3.28		6.94	−2.44	
α-AsN	0.91	−4.98		3.87	−4.25		4.98	−3.11		29.14	−5.75	
α-SbN	1.31	−4.26		7.69	−5.93		7.51	1.21		118.29	−13.20	
α-AsP	0.84	−0.68		2.23	−1.68		2.68	−0.25		18.90	−4.74	
α-SbP	5.86	−0.44		17.73	−9.38		11.00	2.02		142.44	−27.64	
α-SbAs	4.84	−1.70		21.45	−14.73		12.13	3.78		243.45	−63.65	
β- PN	4.36		0.058	3.32		0.033	3.60		−0.15	2.77		−0.088
β-AsN	4.74		0.093	5.64		0.066	4.00		−0.12	4.83		−0.093
β-SbN	5.04		0.063	7.81		0.052	3.16		−0.26	5.30		−0.26
β-AsP	0.60		0.025	1.06		0.031	0.36		0.007	0.67		0.010
β-SbP	1.82		0.046	4.23		0.070	0.86		−0.015	2.26		−0.027
β-SbAs	1.27		0.022	3.36		0.037	0.54		−0.014	1.65		−0.029

Two-dimensional materials which possess giant piezoelectricity have attracted tremendous attention. Besides the most studied *h*-BN and MoS_2, Fei *et al.* reported that the monolayer group-IV monochalcogenides were outstanding 2D piezoelectric materials, i.e., SnSe (d_{11} = 250.58 pm/V) and GeSe (d_{11} = 212.13 pm/V).[13] With the *mm2* symmetry identical to that of monolayer group-IV monochalcogenides, α-phase monolayer group-V binary compounds investigated in this work also exhibit excellent piezoelectric properties. For example, the calculated relaxed-ion coefficients d_{11} of α-SbN, α-SbP, and α-SbAs are 118.29, 142.44, and 243.45 pm/V, respectively, comparable to those of SnSe and GeSe. Although other binary monolayers, i.e., α-PN, α-AsP, and α-AsN, possess relatively small relaxed-ion coefficients d_{11} of 6.94, 18.9, and 29.14 pm/V, respectively, they are still much larger than those of MoS_2 (d_{11} = 3.73 pm/V).[12] The relaxed-ion piezoelectric coefficients d_{11} of different 2D materials are shown in Figure 4a. On the other hand,

although the anisotropic piezoelectric properties have been predicted and discussed in other 2D models,[13, 21] the piezoelectric effect in α-phase monolayer is found to be extremely anisotropic, manifesting itself by a large gap between the absolute values of coefficients d_{11} and d_{12}. These anisotropic behaviors may be useful in the design of nano-sized sensors and energy harvesting devices with special demands.

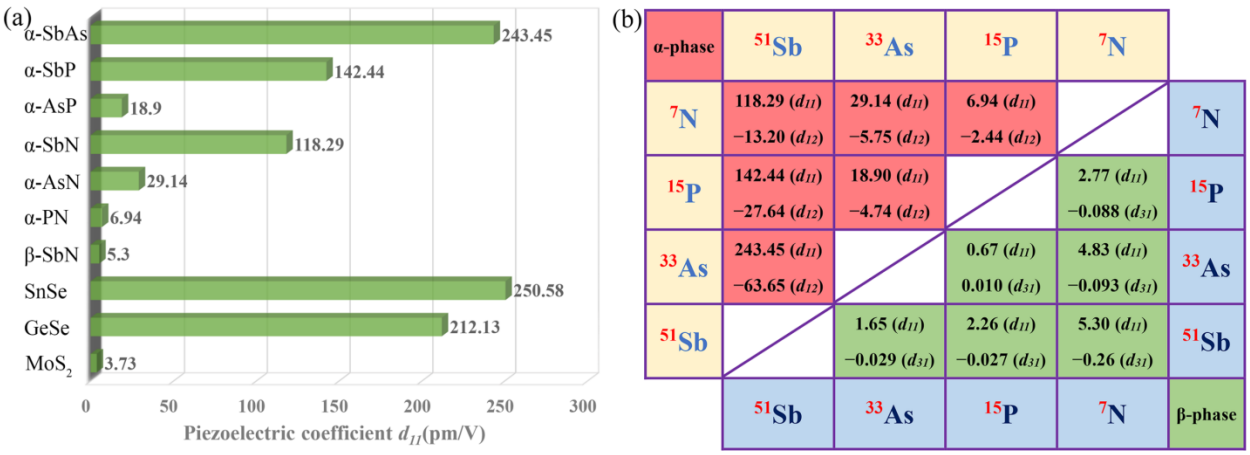

Figure 4. (a) Comparison of the relaxed-ion piezoelectric coefficients d_{11} between previously studied 2D piezoelectric crystals (MoS_2, GeSe, and SnSe) and group-V binary compounds presented in this work. (b) Periodic trends of relaxed-ion piezoelectric coefficients d_{11}, d_{12}, and d_{31} with respect to the order of atomic number for α-phase and β-phase group-V binary monolayers.

The piezoelectric responses in a lot of 2D piezoelectric materials, particularly in those that have elements belonging to the same family, were found to obey a periodic trend.[10, 12-13, 18] As expected, we also find the obvious periodic trend of relaxed-ion piezoelectric coefficients d_{11}, d_{12},

and d_{31} of both α-phase and β-phase group-V binary monolayers. However, as depicted in Figure 4b, the trends for the α-phase and β-phase structures are similar but not exactly the same. Taking nitrides as examples, the piezoelectric coefficients d_{11} and d_{12} for α-phase structures and d_{11} and d_{31} for β-phase structures increase with increasing atomic number of elements, i.e., from PN to AsN, and SbN. Nevertheless, for antimonide, the piezoelectric effects increase gradually with increasing atomic number of elements, i.e., from α-SbN to α-SbP, and α-SbAs, but decrease with increasing atomic number of elements, i.e., from β-SbN to β-SbP, and β-SbAs.

To explore the origin of piezoelectricity of 2D monolayers and explain the mechanism of the periodic trend, Blonsky *et al.* predicted the piezoelectric coefficients of a series of 2D materials, including TMDCs and group-III-V compounds.[10] They proposed a crucial correlation of piezoelectric coefficients d_{11} with atomic polarizabilities, Bader charges and lattice parameters by fitting an empirical formula. Such correlation theory is employed to analyze the trend of piezoelectricity in β-phase group-V binary compounds investigated in this work. The ratio of atomic polarizabilities, which is one of the dominant factors that characterize the piezoelectricity of some 2D compounds, [10] are found to follow the sequence of AsP (1.20) < SbAs (1.42) < SbP (1.69) < PN (3.36) < AsN (4.02) < SbN (5.68), where the reported atomic polarizabilities of N, P, As, and Sb atoms are 7.41, 24.9, 29.8 and 42.2 a.u., respectively.[62] As shown in Figure 4b, the piezoelectric coefficients d_{11} of β-phase monolayers, i.e., β-AsP (0.67 pm/V) < β-SbAs (1.65 pm/V) < β-SbP (2.26 pm/V) < β-PN (2.77 pm/V) < β-AsN (4.83 pm/V) < β-SbN (5.30 pm/V), obviously follow the increases in their corresponding ratio of atomic polarizabilities. Therefore, it is suggested that the piezoelectric responses in β-phase group-V binary compounds are mainly attributed to the distinction of atomic polarizabilities of elements, consistent with those previously predicted in TMDCs monolayers.[10]

For α-phase structures, however, the piezoelectric coefficients d_{11} and d_{12} do not simply controlled by the ratio of atomic polarizabilities. Based on previous studies, for some 2D systems subjected to external uniaxial strains, not only the polarization change but also the displacement of ions should be considered in evaluating the piezoelectric responses.[10-11, 13] Because of the flexile puckered structures for α-phase monolayers, it is speculated that the displacement of ions may play a more dominant role in piezoelectric responses than the atomic polarizabilities, demonstrating by the fact that the piezoelectric coefficients d_{11} (118−243 pm/V) of α-SbN, α-SbP, and α-SbAs monolayers are extremely high. Similarly, owing to the strain-induced ionic motion, the large relaxation contributions to the piezoelectric coefficients in TMDCs were also discussed by Alyörük *et al.*.[63] As a consequence, the previously reported measure on the piezoelectricity in hexagonal structures with a *3m* symmetry,[10-11] i.e., $d_{11} = c_1\frac{\alpha_1}{\alpha_2} + c_2 a_0 Q_B$, which is an empirical correlations between piezoelectric coefficients and atomic polarizabilities, structural properties, and Bader charges, may be inapplicable or only partially fits for α-phase group-V binary compounds because of the tremendous differences (by about two orders of magnitude) in piezoelectric properties of systems changing from α-PN to α-SbAs. Thus, more systematic studies on α-phase structures with an *mm2* symmetry, i.e., group-IV monochalcogenides (SnSe, SnS, GeSe, and GeS)[13] and group-V binary compounds proposed here, would be needed to explore the mechanisms of their giant piezoelectricity.

Two-dimensional piezoelectric materials are very promising in mechanical-to-electrical energy conversion whose conversion efficiency is often decided by their dominant piezoelectric coefficients, such as d_{11} in many systems. The remarkable and anisotropic piezoelectricity reported in this work will promote the applications of α-phase monolayers of group-V binary compounds in the energy harvesting devices. Besides α-phase and β-phase, other seven potential

allotropes, labeled as γ-, δ-, ε-, ζ-, η-, θ-, and ι-phases, respectively, for group-V one-element monolayers (phosphorene, arsenene, and antimonene) have been predicted theoretically by Zhang *et al.*.[29] Subsequently, they have also examined the stabilities and electronic properties of the allotropes of AsP and SbAs binary compounds, including α-, β-, γ-, δ-, and ε-phases.[37, 41] Based on our studies on giant piezoelectricity in this work, it is expected that other non-centrosymmetric phases, beyond α-phase and β-phase, of monolayer group-V binary compounds may be stable or metastable and also exhibit enhanced intrinsic piezoelectricity.

CONCLUSIONS

Based on first-principles DFT calculations, we have systematically examined the piezoelectric effects in 2D monolayer group-V binary compounds with stable honeycomb phases (α-phase and β-phase), including PN, AsN, SbN, AsP, SbP, and SbAs. We find that the group-V binary compounds under study exhibit piezoelectricity, which strongly depends on their structural symmetry. The piezoelectric coefficients of α-phase monolayers are remarkably 1 or 2 orders of magnitude larger than those of the corresponding β-phase monolayers. Notably, the three antimonides, i.e., α-SbN, α-SbP, and α-SbAs, have ultra-high relaxed-ion piezoelectric coefficients d_{11} of 118.29, 142.44, and 243.45 pm/V, respectively, comparable to the recently reported d_{11} of 75-250 pm/V in group-IV monochalcogenides (SnSe, SnS, GeSe, and GeS). Meanwhile, the piezoelectric responses in α-phase monolayers are found to be obviously anisotropic. Furthermore, the periodic trend in the piezoelectric properties of β-phase monolayers is demonstrated to depend on the atomic polarizabilities. While for α-phase monolayers, the origin of giant piezoelectricity becomes confusing and more parameters of mechanical and

electronic properties need to be considered comprehensively. From the theoretical calculations, we have gained an unrivalled understanding of the piezoelectricity in 2D group-V binary compounds, which would facilitate the optimization on these novel materials for their applications in flexible sensors and energy conversion devices.

AUTHOR INFORMATION

Corresponding Author

*E-mail: mmzheng@polyu.edu.hk

*E-mail: wangyx@henu.edu.cn

Notes

The authors declare no competing financial interest.

ACKNOWLEDGMENT

This work was supported by the National Natural Science Foundation of China (Grants Nos. 21603056, 11674083, 21433006, and 21573131), the Hong Kong Scholars Program (XJ2016045), the Project of Scientific Research Fund in Henan University (YQPY20170076), the Fundamental and Advanced Technology Research Project in Henan Province (162300410224), and a grant from the Research Grants Council of the Hong Kong Special Administrative Region, China (PolyU 152607/16E).

REFERENCES

1. Novoselov, K. S.; Geim, A. K.; Morozov, S. V.; Jiang, D.; Zhang, Y.; Dubonos, S. V.; Grigorieva, I. V.; Firsov, A. A. Electric Field Effect in Atomically Thin Carbon Films. *Science* **2004**, *306*, 666-669.
2. Xu, M.; Liang, T.; Shi, M.; Chen, H. Graphene-Like Two-Dimensional Materials. *Chem. Rev.* **2013**, *113*, 3766-3798.
3. Bhimanapati, G. R.; Lin, Z.; Meunier, V.; Jung, Y.; Cha, J.; Das, S.; Xiao, D.; Son, Y.; Strano, M. S.; Cooper, V. R.; et al. Recent Advances in Two-Dimensional Materials Beyond Graphene. *ACS Nano* **2015**, *9*, 11509-11539.
4. Xia, F.; Wang, H.; Xiao, D.; Dubey, M.; Ramasubramaniam, A. Two-Dimensional Material Nanophotonics. *Nat. Photon.* **2014**, *8*, 899-907.
5. Fiori, G.; Bonaccorso, F.; Iannaccone, G.; Palacios, T.; Neumaier, D.; Seabaugh, A.; Banerjee, S. K.; Colombo, L. Electronics Based on Two-Dimensional Materials. *Nat. Nanotechnol.* **2014**, *9*, 768-779.
6. Michel, K. H.; Verberck, B. Theory of Elastic and Piezoelectric Effects in Two-Dimensional Hexagonal Boron Nitride. *Phys. Rev. B* **2009**, *80*, 224301.
7. Wu, W.; Wang, L.; Li, Y.; Zhang, F.; Lin, L.; Niu, S.; Chenet, D.; Zhang, X.; Hao, Y.; Heinz, T. F.; et al. Piezoelectricity of Single-Atomic-Layer MoS_2 for Energy Conversion and Piezotronics. *Nature* **2014**, *514*, 470-474.
8. Zhu, H.; Wang, Y.; Xiao, J.; Liu, M.; Xiong, S.; Wong, Z. J.; Ye, Z.; Ye, Y.; Yin, X.; Zhang, X. Observation of Piezoelectricity in Free-Standing Monolayer MoS_2. *Nat. Nanotechnol.* **2015**, *10*, 151-155.
9. Ong, M. T.; Reed, E. J. Engineered Piezoelectricity in Graphene. *ACS Nano* **2012**, *6*, 1387-1394.
10. Blonsky, M. N.; Zhuang, H. L.; Singh, A. K.; Hennig, R. G. Ab Initio Prediction of Piezoelectricity in Two-Dimensional Materials. *ACS Nano* **2015**, *9*, 9885-9891.
11. Sevik, C.; Çakır, D.; Gülseren, O.; Peeters, F. M. Peculiar Piezoelectric Properties of Soft Two-Dimensional Materials. *J. Phys. Chem. C* **2016**, *120*, 13948-13953.
12. Duerloo, K.-A. N.; Ong, M. T.; Reed, E. J. Intrinsic Piezoelectricity in Two-Dimensional Materials. *J. Phys. Chem. Lett.* **2012**, *3*, 2871-2876.
13. Fei, R.; Li, W.; Li, J.; Yang, L. Giant Piezoelectricity of Monolayer Group IV Monochalcogenides: SnSe, SnS, GeSe, and GeS. *Appl. Phys. Lett.* **2015**, *107*, 173104.
14. Michel, K. H.; Verberck, B. Phonon Dispersions and Piezoelectricity in Bulk and Multilayers of Hexagonal Boron Nitride. *Phys. Rev. B* **2011**, *83*, 115328.
15. Alyörük, M. M. Piezoelectric Properties of Monolayer II–VI Group Oxides by First-Principles Calculations. *Phys. Status Solidi B* **2016**, *253*, 2534-2539.
16. Li, W.; Li, J. Piezoelectricity in Two-Dimensional Group-III Monochalcogenides. *Nano Res.* **2015**, *8*, 3796-3802.
17. Guo, Y.; Zhou, S.; Bai, Y.; Zhao, J. Enhanced Piezoelectric Effect in Janus Group-III Chalcogenide Monolayers. *Appl. Phys. Lett.* **2017**, *110*, 163102.
18. Gao, R.; Gao, Y. Piezoelectricity in Two-Dimensional Group III–V Buckled Honeycomb Monolayers. *Phys. Status Solidi RRL* **2017**, *11*, 1600412.
19. Bechmann, R. Elastic and Piezoelectric Constants of Alpha-Quartz. *Phys. Rev.* **1958**, *110*, 1060-1061.
20. Lueng, C. M.; Chan, H. L. W.; Surya, C.; Choy, C. L. Piezoelectric Coefficient of Aluminum Nitride and Gallium Nitride. *J. Appl. Phys.* **2000**, *88*, 5360-5363.

21. Hu, T.; Dong, J. Two New Phases of Monolayer Group-IV Monochalcogenides and Their Piezoelectric Properties. *Phys. Chem. Chem. Phys.* **2016**, *18*, 32514-32520.
22. Li, L.; Yu, Y.; Ye, G. J.; Ge, Q.; Ou, X.; Wu, H.; Feng, D.; Chen, X. H.; Zhang, Y. Black Phosphorus Field-Effect Transistors. *Nat. Nanotechnol.* **2014**, *9*, 372-377.
23. Liu, H.; Neal, A. T.; Zhu, Z.; Luo, Z.; Xu, X.; Tománek, D.; Ye, P. D. Phosphorene: An Unexplored 2d Semiconductor with a High Hole Mobility. *ACS Nano* **2014**, *8*, 4033-4041.
24. Yasaei, P.; Kumar, B.; Foroozan, T.; Wang, C.; Asadi, M.; Tuschel, D.; Indacochea, J. E.; Klie, R. F.; Salehi-Khojin, A. High-Quality Black Phosphorus Atomic Layers by Liquid-Phase Exfoliation. *Adv. Mater.* **2015**, *27*, 1887-1892.
25. Kamal, C.; Ezawa, M. Arsenene: Two-Dimensional Buckled and Puckered Honeycomb Arsenic Systems. *Phys. Rev. B* **2015**, *91*, 085423.
26. Wang, Y.; Ye, M.; Weng, M.; Li, J.; Zhang, X.; Zhang, H.; Guo, Y.; Pan, Y.; Xiao, L.; Liu, J.; et al. Electrical Contacts in Monolayer Arsenene Devices. *ACS Appl. Mater. Interfaces* **2017**, *9*, 29273-29284
27. Zhu, Z.; Guan, J.; Tománek, D. Strain-Induced Metal-Semiconductor Transition in Monolayers and Bilayers of Gray Arsenic: A Computational Study. *Phys. Rev. B* **2015**, *91*, 161404.
28. Zhang, S.; Yan, Z.; Li, Y.; Chen, Z.; Zeng, H. Atomically Thin Arsenene and Antimonene: Semimetal–Semiconductor and Indirect–Direct Band-Gap Transitions. *Angew. Chem. Int. Ed.* **2015**, *54*, 3112-3115.
29. Zhang, S.; Xie, M.; Li, F.; Yan, Z.; Li, Y.; Kan, E.; Liu, W.; Chen, Z.; Zeng, H. Semiconducting Group 15 Monolayers: A Broad Range of Band Gaps and High Carrier Mobilities. *Angew. Chem. Int. Ed.* **2016**, *55*, 1666-1669.
30. Pumera, M.; Sofer, Z. 2D Monoelemental Arsenene, Antimonene, and Bismuthene: Beyond Black Phosphorus. *Adv. Mater.* **2017**, *29*, 1605299.
31. Gibaja, C.; Rodriguez-San-Miguel, D.; Ares, P.; Gómez-Herrero, J.; Varela, M.; Gillen, R.; Maultzsch, J.; Hauke, F.; Hirsch, A.; Abellán, G.; et al. Few-Layer Antimonene by Liquid-Phase Exfoliation. *Angew. Chem. Int. Ed.* **2016**, *55*, 14345-14349.
32. Ares, P.; Aguilar-Galindo, F.; Rodríguez-San-Miguel, D.; Aldave, D. A.; Díaz-Tendero, S.; Alcamí, M.; Martín, F.; Gómez-Herrero, J.; Zamora, F. Mechanical Isolation of Highly Stable Antimonene under Ambient Conditions. *Adv. Mater.* **2016**, *28*, 6332-6336.
33. Xie, M.; Zhang, S.; Cai, B.; Gu, Y.; Liu, X.; Kan, E.; Zeng, H. Van Der Waals Bilayer Antimonene: A Promising Thermophotovoltaic Cell Material with 31% Energy Conversion Efficiency. *Nano Energy* **2017**, *38*, 561-568.
34. Wang, G.; Pandey, R.; Karna, S. P. Atomically Thin Group V Elemental Films: Theoretical Investigations of Antimonene Allotropes. *ACS Appl. Mater. Interfaces* **2015**, *7*, 11490-11496.
35. Tsai, H.-S.; Wang, S.-W.; Hsiao, C.-H.; Chen, C.-W.; Ouyang, H.; Chueh, Y.-L.; Kuo, H.-C.; Liang, J.-H. Direct Synthesis and Practical Bandgap Estimation of Multilayer Arsenene Nanoribbons. *Chem. Mater.* **2016**, *28*, 425-429.
36. Zhu, Z.; Guan, J.; Tománek, D. Structural Transition in Layered $As_{1-x}P_x$ Compounds: A Computational Study. *Nano Lett.* **2015**, *15*, 6042-6046.
37. Xie, M.; Zhang, S.; Cai, B.; Huang, Y.; Zou, Y.; Guo, B.; Gu, Y.; Zeng, H. A Promising Two-Dimensional Solar Cell Donor: Black Arsenic–Phosphorus Monolayer with 1.54 eV Direct Bandgap and Mobility Exceeding 14,000 $cm^2 V^{-1} s^{-1}$. *Nano Energy* **2016**, *28*, 433-439.

38. Liu, B.; Köpf, M.; Abbas, A. N.; Wang, X.; Guo, Q.; Jia, Y.; Xia, F.; Weihrich, R.; Bachhuber, F.; Pielnhofer, F.; et al. Black Arsenic–Phosphorus: Layered Anisotropic Infrared Semiconductors with Highly Tunable Compositions and Properties. *Adv. Mater.* **2015**, *27*, 4423-4429.
39. Kou, L.; Ma, Y.; Tan, X.; Frauenheim, T.; Du, A.; Smith, S. Structural and Electronic Properties of Layered Arsenic and Antimony Arsenide. *J. Phys. Chem. C* **2015**, *119*, 6918-6922.
40. Liu, P.; Nie, Y.-Z.; Xia, Q.-L.; Guo, G.-H. Structural and Electronic Properties of Arsenic Nitrogen Monolayer. *Phys. Lett. A* **2017**, *381*, 1102-1106.
41. Zhang, S.; Xie, M.; Cai, B.; Zhang, H.; Ma, Y.; Chen, Z.; Zhu, Z.; Hu, Z.; Zeng, H. Semiconductor-Topological Insulator Transition of Two-Dimensional SbAs Induced by Biaxial Tensile Strain. *Phys. Rev. B* **2016**, *93*, 245303.
42. Nie, Y.; Rahman, M.; Liu, P.; Sidike, A.; Xia, Q.; Guo, G.-H. Room-Temperature Half-Metallicity in Monolayer Honeycomb Structures of Group-V Binary Compounds with Carrier Doping. *Phys. Rev. B* **2017**, *96*, 075401.
43. Cai, B.; Xie, M.; Zhang, S.; Huang, C.; Kan, E.; Chen, X.; Gu, Y.; Zeng, H. A Promising Two-Dimensional Channel Material: Monolayer Antimonide Phosphorus. *Sci. China Mater.* **2016**, *59*, 648-656.
44. Li, S.-S.; Ji, W.-X.; Li, P.; Hu, S.-J.; Zhou, T.; Zhang, C.-W.; Yan, S.-S. Unconventional Band Inversion and Intrinsic Quantum Spin Hall Effect in Functionalized Group-V Binary Films. *Sci. Rep.* **2017**, *7*, 6126.
45. Nie, Y.; Rahman, M.; Wang, D.; Wang, C.; Guo, G. Strain Induced Topological Phase Transitions in Monolayer Honeycomb Structures of Group-V Binary Compounds. *Sci. Rep.* **2015**, *5*, 17980.
46. Yu, W.; Niu, C.-Y.; Zhu, Z.; Wang, X.; Zhang, W.-B. Atomically Thin Binary V-V Compound Semiconductor: A First-Principles Study. *J. Mater. Chem. C* **2016**, *4*, 6581-6587.
47. Xiao, H.; Hao, F.; Liao, X.; Shi, X.; Zhang, Y.; Chen, X. Prediction of a Two-Dimensional Phosphorus Nitride Monolayer. *arXiv:1603.01957* **2016**.
48. Zhang, Q.; Schwingenschlögl, U. Emergence of Dirac and Quantum Spin Hall States in Fluorinated Monolayer As and AsSb. *Phys. Rev. B* **2016**, *93*, 045312.
49. Kresse, G.; Furthmüller, J. Efficiency of Ab-Initio Total Energy Calculations for Metals and Semiconductors Using a Plane-Wave Basis Set. *Comput. Mater. Sci.* **1996**, *6*, 15-50.
50. Kresse, G.; Furthmüller, J. Efficient Iterative Schemes for Ab Initio Total-Energy Calculations Using a Plane-Wave Basis Set. *Phys. Rev. B* **1996**, *54*, 11169-11186.
51. Kresse, G.; Joubert, D. From Ultrasoft Pseudopotentials to the Projector Augmented-Wave Method. *Phys. Rev. B* **1999**, *59*, 1758-1775.
52. Perdew, J. P.; Burke, K.; Ernzerhof, M. Generalized Gradient Approximation Made Simple. *Phys. Rev. Lett.* **1996**, *77*, 3865-3868.
53. Monkhorst, H. J.; Pack, J. D. Special Points for Brillouin-Zone Integrations. *Phys. Rev. B* **1976**, *13*, 5188-5192.
54. Wu, X.; Vanderbilt, D.; Hamann, D. R. Systematic Treatment of Displacements, Strains, and Electric Fields in Density-Functional Perturbation Theory. *Phys. Rev. B* **2005**, *72*, 035105.
55. King-Smith, R. D.; Vanderbilt, D. Theory of Polarization of Crystalline Solids. *Phys. Rev. B* **1993**, *47*, 1651-1654.
56. Vanderbilt, D. Berry-Phase Theory of Proper Piezoelectric Response. *J. Phys. Chem. Solids* **2000**, *61*, 147-151.

57. Nye, J. F. *Physical Properties of Crystals: Their Representation by Tensors and Matrices*; Oxford University Press: New York, USA, 1985.
58. Hybertsen, M. S.; Louie, S. G. First-Principles Theory of Quasiparticles: Calculation of Band Gaps in Semiconductors and Insulators. *Phys. Rev. Lett.* **1985**, *55*, 1418-1421.
59. Heyd, J.; Scuseria, G. E.; Ernzerhof, M. Erratum: "Hybrid Functionals Based on a Screened Coulomb Potential" [J. Chem. Phys. 118, 8207 (2003)]. *J. Chem. Phys.* **2006**, *124*, 219906.
60. Kecik, D.; Durgun, E.; Ciraci, S. Stability of Single-Layer and Multilayer Arsenene and Their Mechanical and Electronic Properties. *Phys. Rev. B* **2016**, *94*, 205409.
61. Wang, Y.; Ding, Y. Unexpected Buckled Structures and Tunable Electronic Properties in Arsenic Nanosheets: Insights from First-Principles Calculations. *J. Phys.: Condens. Matter* **2015**, *27*, 225304.
62. Roos, B. O.; Lindh, R.; Malmqvist, P.-Å.; Veryazov, V.; Widmark, P.-O. Main Group Atoms and Dimers Studied with a New Relativistic ANO Basis Set. *J. Phys. Chem. A* **2004**, *108*, 2851-2858.
63. Alyörük, M. M.; Aierken, Y.; Çakır, D.; Peeters, F. M.; Sevik, C. Promising Piezoelectric Performance of Single Layer Transition-Metal Dichalcogenides and Dioxides. *J. Phys. Chem. C* **2015,** *119*, 23231-23237.

TOC Graphic

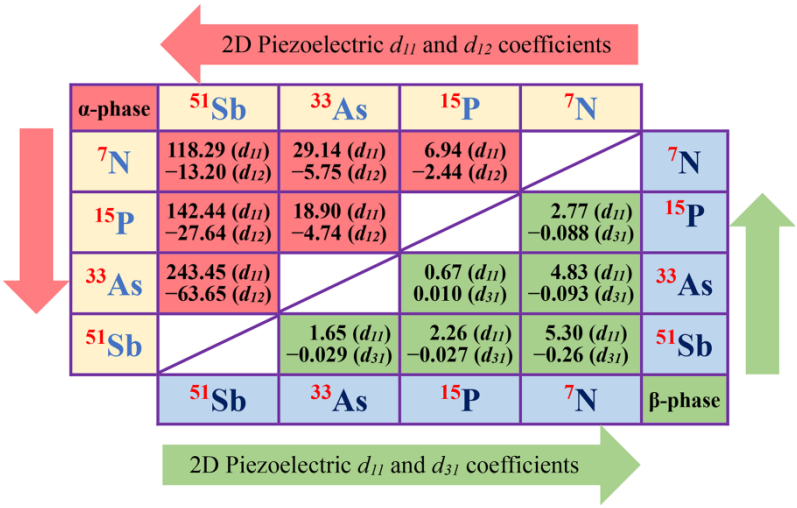
2D Piezoelectric d_{11} and d_{12} coefficients
α-phase
^{51}Sb
^{33}As
^{15}P
^{7}N
^{7}N
118.29 (d_{11}) −13.20 (d_{12})
29.14 (d_{11}) −5.75 (d_{12})
6.94 (d_{11}) −2.44 (d_{12})
^{7}N
^{15}P
142.44 (d_{11}) −27.64 (d_{12})
18.90 (d_{11}) −4.74 (d_{12})
2.77 (d_{11}) −0.088 (d_{31})
^{15}P
^{33}As
243.45 (d_{11}) −63.65 (d_{12})
0.67 (d_{11}) 0.010 (d_{31})
4.83 (d_{11}) −0.093 (d_{31})
^{33}As
^{51}Sb
1.65 (d_{11}) −0.029 (d_{31})
2.26 (d_{11}) −0.027 (d_{31})
5.30 (d_{11}) −0.26 (d_{31})
^{51}Sb
^{51}Sb
^{33}As
^{15}P
^{7}N
β-phase
2D Piezoelectric d_{11} and d_{31} coefficients